A Dynamic Model for Series and Parallel Resistance of Photovoltaic Cell using Material Properties Extraction and Energy Tunnel

Kotchapong Sumanonta[*1],
Pasist Suwanapingkarl[**2], and **Pisit Liutanakul**[*3], Non-members

ABSTRACT

This article presents a novel model for the equivalent circuit of a photovoltaic module. This circuit consists of the following important parameters: a single diode, series resistance (R_s) and parallel resistance (R_p) that can be directly adjusted according to ambient temperature and the irradiance. The single diode in the circuit is directly related to the ideality factor (m), which represents the relationship between the materials and significant structures of PV module such as mono-crystalline, multi-crystalline and thin-film technology. Specifically, the proposed model in this article is to present the simplified model that can calculate the results of I-V curves faster and more accurate than other methods of the previous models. This can show that the proposed models are more suitable for the practical application.In addition, the results of the proposed model are validated by the datasheet, the practical data in the laboratory (indoor test) and the onsite data (outdoor test). This ensures that the less than 0.1% absolute errors of the model can be accepted.

Keywords: Dynamic programming Photovoltaic cells, Silicon, Thin-film.

1. INTRODUCTION

Nowadays, the demand for energy continually increases, while the energy resources, such as conventional fuel dramatically decreases. Therefore, the alternative energy resources are needed during high energy demand for sufficient amounts of energy. Direct Current (D.C.) which is supplied from Photovoltaic (PV) modules is considered, as one of the clean alternative energies, which does not pollute the environment. It is well known that the performance of PV modules generally depend on irradiance (G_a) in W/m^2 and ambient temperature (T_a) in ^{o}C, which can change the generated power over time. In general, the PV manufacturer usually provides the characteristic current-voltage curve (I-V curve) of PV module in non-linear relationship [1].As presented in the standard test condition (STC) in Fig. 1, one can observe that there are 4 important parameters, which are : the open-circuit voltage under standard test condition in voltages ($V_{oc,stc}$), the short-circuit current under standard test condition in amperes ($I_{sc,stc}$), the maximum power point voltage under standard test condition ($V_{mpp,stc}$) and the maximum power point current under standard test condition ($I_{mpp,stc}$) respectively. In general, the PV manufacturer usually provides a few technical parameters, such as the coefficient values of the open-circuit voltage (k_v) and the coefficient values of the short-circuit current (k_i) under standard test conditions, respectively.

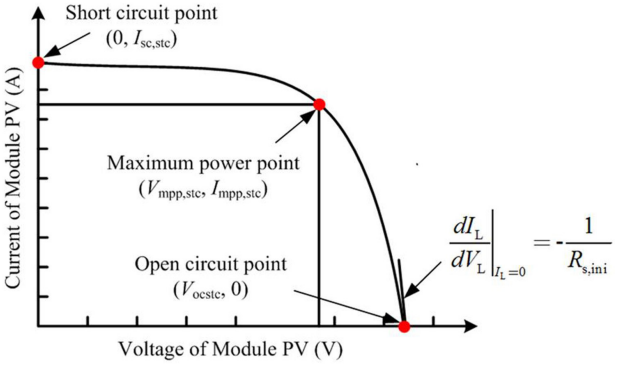

Fig. 1: *I-V Curve of PV module.*

Thus, an equivalent circuit model that precisely predicts the behavior of generated power for every condition of irradiance and ambient temperature is required in order to model PV cells. Hence, the 4 typical general mathematical models of PV modules are shown in Fig. 2. Where, I_l means the generated current in photovoltaic module due to solar irradiance (A), R_s equals to the series resistance (Ω), R_p describes the parallel resistance (Ω) and d means the diode, respectively.

Recently, the several mathematical models of PV are illustrated to the equivalent circuits as shown in

Manuscript received on July 30, 2017 ; revised on December 1, 2017.
* The authors are with Department of Electrical and Computer Engineer ing, Faculty of Engineering, King Mongkut's University of Technology North Bangkok (KMUTNB), Bangkok, Thailand, 10800, E-mail : kotchapong01@yahoo.com[1]
** The author is with the Department of Electrical Engineering, Faculty of Engineering at Rajamangala University of Technology Phra-Nakhon, Bangsue, Bangkok, Thailand, 10800.

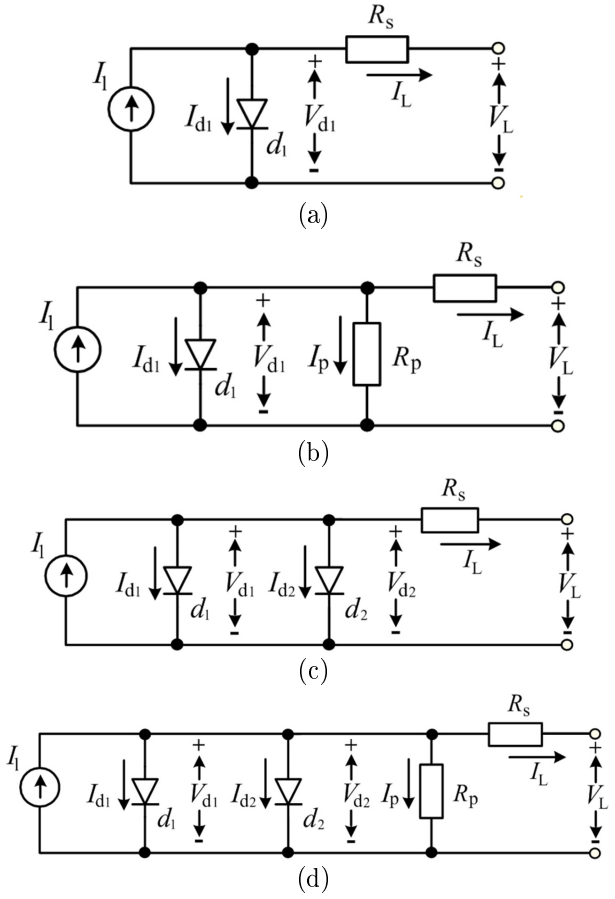

Fig.2: *Equivalent circuit of (a) SDM-1, (b) SDM-2, (c) DDM-1 and (d) DDM-2.*

Fig. 2, for instance, single-diode (SDM) and double-diode models (DDM) [1]. However, the precision of the I-V curve through PV modules depends on the types of the equivalent circuits [2]-[15].

Nevertheless, the SDM-1 in Fig. 2(a), has 4 unknown parameters [2]-[4] such as, the ideality factor of diode (m), saturation current (I_o), I_l and R_s. Also, this model [2] is composed of m and R_s which are varied due to T_a. While, the ideality factor of diode of this model is constant between ($0 \leq m \leq 2$) for the crystalline PV module only, which SDM-1 has been delivered the high relative error from the analytical output power of PV module. Therefore, the SDM-1 is not appropriately utilized for practice.

Furthermore, all the weakness of SDM-1, can be improved through the simulation of single diode model type 2 (SDM-2) as shown in Fig. 2(b), which it is provided with a parallel resistance [5]-[7]. Essentially, the I-V curve of SDM-2, is high precision and more reliable than SDM-1.

Moreover, the SDM-1 was updated to the double diode model type 1 (DDM-1) with a series resistance as shown in Fig. 2(c) [8], [9]. Hence, this model delivers high precision result of the I-V curve. However, it had a complicated problem for analysis of the I-V curve, because both diode current is nonlinear relationship.

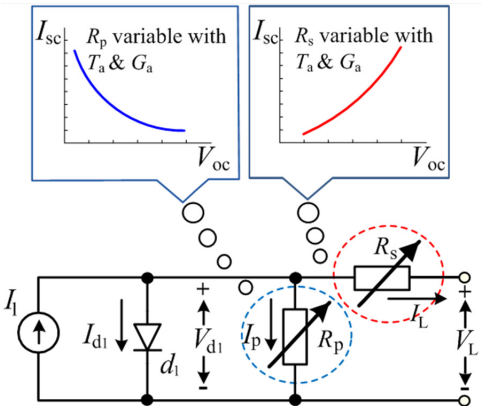

Fig.3: *The proposed model for pv module.*

The equivalent circuit in Fig. 2(d), is the double diode model type 2 (DDM-2) with additional parallel resistance. Also, it can be generated the high accurate result more than DDM-1. However, the calculated process of DDM-2 was extremely complicated [10-12], also the equivalent circuits have more unknown parameters than other models [4].

Nevertheless, all the models were illustrated in Fig. 2, haven't been analyzed to consider through extensive variations of the unknown parameters in real time [2] - [12]. Although, many researchers [7], [13]-[15] have applied extraction methods to design the simulate PV models to get more accurate on the I-V curve.

As mentioned above, the SDM-1 has a low accuracy result. While, the SDM-2, DDM-1, DDM-2 have been complicated and various limitations for estimating result. Therefore, these models are not appropriate for implementation. Nowadays, the many constraints of the existing equivalent circuit are not improved. Hence, the modern mathematical model is proposed for the PV module as shown in Fig.3.

According to Fig.3, the proposed model is demonstrated in a single diode equivalent circuit with the adjustable series and parallel resistance. Hence, the Rs and Rp can be varied under environment condition (e.g. irradiance (G_a), ambient temperature (T_a) and operating temperature of the PV). Also, the ideality factor (m) in the proposed model, has been calculated through the physical substance, such as the periodic table and the operating temperature of PV, respectively [16] - [18]. Therefore, the significant parameters of the proposed model as m, R_s and R_p, are defined at the real time condition.

Essentially, the prominent point of the proposed model is more beneficial and realistic than the existing PV models (SDM-1, SDM-2, DDM-1 and DDM-2). These existing models are almost utilized on the commercial programs, such as, Matlab-Simulink. Also, the many parameters of the existing PV models as R_s, R_p and m, are not proportional to T_a and

G_a [6]-[12], that are not realistic for implementation. Therefore, the analytical result of the proposed model can be delivered higher precision than the general model of commercial programs.

Besides, the proposed model accuracy is confirmed the accuracy through comparison with the manufactured technical data sheet, namely, Bosch, Photowatt and Sharp. As a result, the solution of the proposed model extremely corresponds with the technical data sheet. Furthermore, the proposed model can demonstrate the high accurate maximum power point (MPP), as well as, it can be analyzed to determine the fast convergent solution, due to having lower constraints than the existing equivalent circuit.

Finally, this proposed model can be demonstrated to apply to the indoor test of Crystalline and Thin Film technology of PV modules, respectively.

The remainder of this paper is organized as follows. The mathematical concept of the proposed model is presented in Section 2 of this paper, the results of the proposed models are compared with the experimental results and PV manufacturer datasheet in Section 3, the conclusion and suggestions are then presented in Section 4, respectively.

2. CHARACTERISTIC OF THE PV CELL

Generally, the PV cell can absorb the photons from the solar irradiation. Also, these photons provide their energy, which is an excited and separated process within the bond. Which is composed of the generating electrons and holes at the surrounding atom and ions in the P and N regions (consider as conductive regions) [19].

Essentially, require the concept of PV cell. "under the illumination", the main current occurs through the photocurrent. Also, this result is directly concerned with the minority carriers. Therefore, the collected electrons in N region can move to the front metal contact, whereas, the existing collected holes in the P region, must be moved to the back metal contact of PV cell, respectively. Besides, the photocurrent can be deduced by diode current, which is generates current to the electrical load.

Although, at the boundary between the P and N regions, the electric field occurs. Also, the diffuseness of the free electrons and holes can move into the opposite region. Therefore, the hole with negative acceptor ions in the P region and the free electron with positive donor ions in the N-region occur [19], [20]. Also, this process occurs during the equilibrium condition or illumination, where the built-in electric field or built-in electric voltage drops across the P-N junction as shown in Fig.4.

According to the Fig. 4, the P-N junction (or space charge region or depletion region) can be described, as follows: the non-conductive region, has the significant contribution area and the rectification process, which it can move the electrons and holes to the opposite side. Due to the losses in N and P regions, their charges become neutral [21], [22]. Hence, the electricity can be produced by the external load connected across the P and N regions of a solar cell, respectively. Moreover, the P-N region behaves as an ideal diode, this allows the free electrons to flow through this connection to the positive holes and lights up the lamp, which is similar to the battery as shown Fig.5.

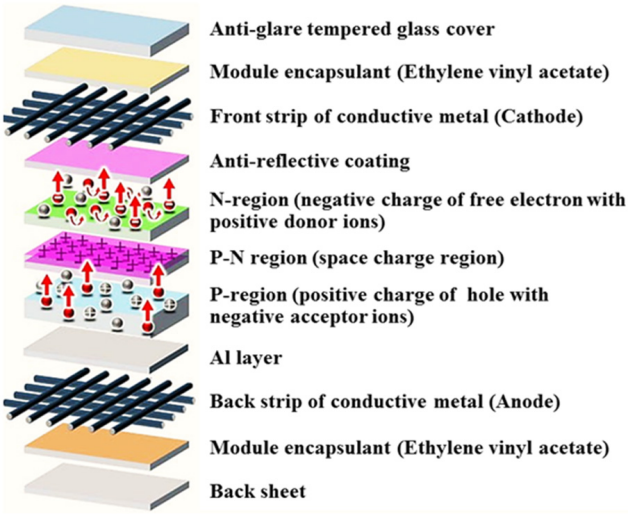

Fig.4: *Typical PV cell structure.*

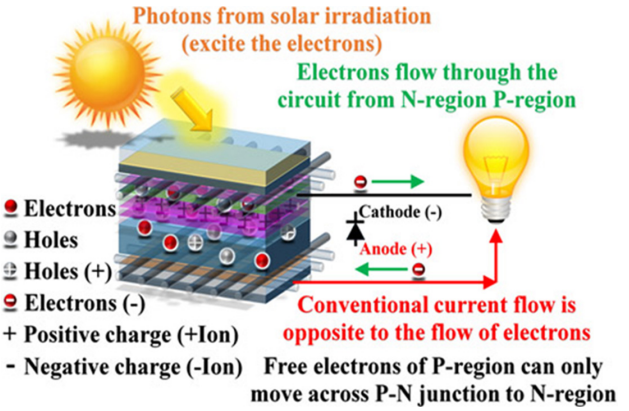

Fig.5: *Current flow in PV cell.*

As mentioned above, this paper proposes the dynamic generic PV model for the crystalline and thin-film technologies, which allows for real-time input data of solar irradiation (W/m^2) and ambient temperature (^oC), respectively. Moreover, the model of this paper is considered the impacts of the electron potential energy between junctions, R_s and R_p.

2.1 Energy tunneling and ideality factor

It is well known that the electrostatic potential in the wafer of PV cell (ψ), it produces the total charge density due to the impurities varies with position. That means the electrons and holes, should be able to distribute themselves so that equilibrium

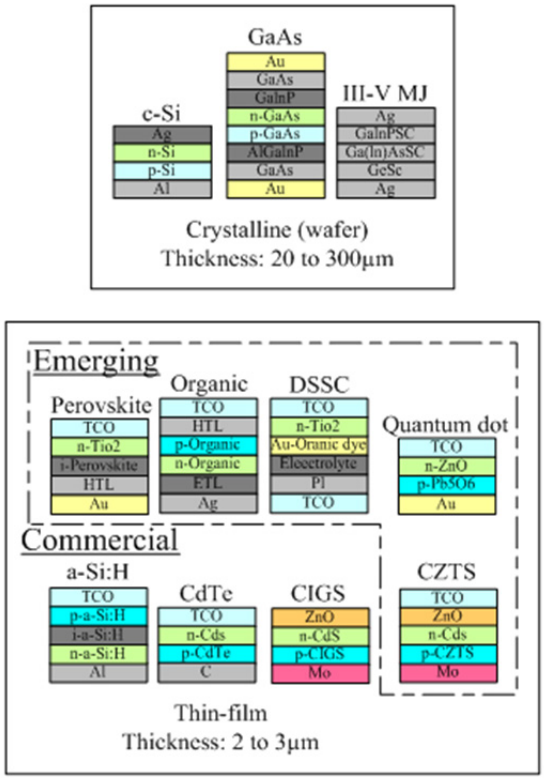

Fig.6: *PV cell structure for the crystalline and thin-film technologies.*

is produced, and hence there will be an unbalanced charge throughout the junction. The concentrations of density between ionized donors (N_d) and ionized acceptors (N_a) can be specified by trivalent impurities region (called P-region) and pentavalent impurities layer (called N-region). Thus, the flow of electrons and holes must be considered in both regions. Fig. 6. shows the comparison between the PV cell structure for crystalline and thin-film technologies.

In order to support the dynamic generic PV model for the crystalline and thin-film technologies that have either single or multi-junctions, Thermionic Field Emission [23] the Thermionic Field Emission (TFE) technique is chosen, because it can analyze the performance of the Schottky Barrier (SB) and the conduction phenomena across a SB as well as it can also extract the parameters from the conduction band of the SB [24]. Thus, the ideality factor of the PV cell of each P-N region as (m_n), which this factor occurs due to the impact of the N type semiconductor material. Also, it relates to the tunneling energy [24] on each junction (E_{oo_n}) can be determined by (1)

$$m_n = \left[\frac{(q)\,(E_{oo_n})}{(k)\,(T_c)}\right] \coth\left[\frac{(q)\,(E_{oo_n})}{(k)\,(T_c)}\right] \qquad (1)$$

Where, the electrical charge on the electron (q) is 1.602×10^{-19} C, the Boltzmann's constant (k) is 1.381×10^{-23}J/K and the operating temperature of the PV cell (T_c) in Kelvin (K). Hence, the thermal and physical properties of the cell or module, solar irradiation and weather, heat transfer coefficient are also considered.

Table 1: *Typical INOCT for PV Module.*

PV module mount type	INOCT(°C)
Rack mount	-3
Direct mount	18
Typical standoff/integral	4
Standoff/integral, entrance or exit height/width, Whichever is minimum 2.5 cm	11
Standoff/integral, entrance or exit height/width, Whichever is minimum 7.5 cm	2
Standoff/integral, entrance or exit height/width, Whichever is minimum 15 cm	-1

Consequently, the overall of the heat losses coefficient from the module and mounting configuration, directly affects the performance of the PV cell, especially the T_c. It is known that the operating temperature inside the PV cell is normally a little higher than the rear of the PV module. This is due to the substrate and doping material, construction of the module, mounting installation and ambient temperature.

Hence, the combination of the ambient temperature T_a in Celsius (°C), the Nominal Operating Cell Temperature (NOCT) under solar irradiation 800 W/m^2 at 20°C, Installed Nominal Operating Cell temperature (INOCT), the actual solar irradiation (G_a) in W/m^2 and the solar irradiation under standard test condition (G_{stc}) is 1000 W/m^2 at 25°C are chosen in order to determine the T_c ,which response to the overall heat losses as described in (2) [17], [18].

$$T_c = 273.15 + T_a + \left[\left(\frac{NOCT + INOCT}{0.8}\right)\left(\frac{G_a}{G_{stc}}\right)\right] \qquad (2)$$

The NOCT of the PV module can be found in the manu- facture datasheet and the typical value of the NOCT is 44°C [18], [25] where the INOCT are shown in Table 1.

In addition, the electron normally behaves as a particle with mass, and therefore E_{oo_n} the can be described by:

$$E_{oo_n} = \left(\frac{\bar{h}}{2}\right)\sqrt{\left\{\frac{N_{d,norm}}{[(m_o)\,(m_r)]\,[(\varepsilon_o)\,(\varepsilon_r)]}\right\}} \qquad (3)$$

When, the Planck's constant with angular frequency (or the reduced Planck's constant or Dirac's

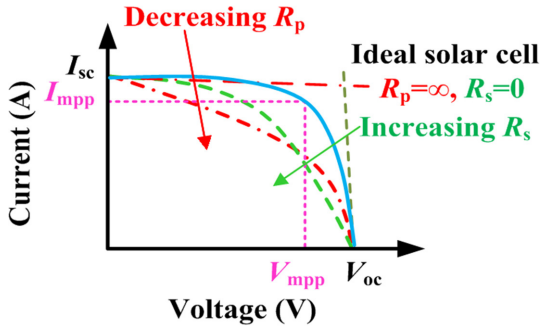

Fig. 7: *Characteristic R_s and R_p of PV cell.*

constant; $\bar{h}$) is 1.0544 $\times 10^{-34}$J.s, the density concentration of the ionized donor ($N_{d,norm}$), the free electron rest mass (m_o) is 9.109$\times 10^{-31}$kg, the effective mass of the donor electron (m_r), the permittivity of free space (absolute permittivity; ε_o) is 8.854$\times 10^{-14}$ F/cm and the relative permittivity or dielectric constant of the donor material (ε_r) .

To support the PV cell with multi-junction, the normalization technique is chosen as this technique supports more sophisticated adjustment of the different scales into the notionally common scale by allowing the entire probability distributions of the different scales into the same alignment [26]. Therefore, the concentration density of ionized donors ($N_{d,norm}$) for multi-junction can be normalized as follows:

$$N_{d,norm} = \frac{N_{d_1} + ... + N_{d_n}}{n} \tag{4}$$

Besides, it can be investigated that the typical values of the N_{d_n} for the PV cell on each P-N region and n equals the total number of concentrations density of ionized donors types [27]-[30]. Consequently, the simplify ideality factor (m_{Tot}) for the PV cell with multi-junction can be evaluated by:

$$m_{Tot} = \frac{m_{n,\max} + ... + m_{n,\min}}{2} \tag{5}$$

Where, the $m_{n,max}$ and $m_{n,min}$ are defined by the maximum and minimum values of the ideality factor that relates to the tunneling energy from the overall junction. It should be noted that the m_{Tot} must be varied within $1 < m_{Tot} < 5$ [25], [31-33].

As can be seen in equations (1) to (5), the ideality factor is inversely proportional to the temperature, where it is proportional to the carrier concentration. That means the ideality factor is found to increase when the decreasing of temperature. While, the ideality factor is increased, when the increasing of carrier concentration [25], [32] and [18], respectively. This is due to the force (force here refers to the occurrence of charge carriers that crosses the junction.) between the upper and lower barrier heights.

2.2 The effects of R_s and R_p

The resistance of the PV cell due to the substrate and doping material, the contact resistance between contacts and materials, the resistance between contact and interconnections (or junction) are normally considered as R_s parameter [1], [34], and [35] where the leakage current that flows as the proportional function of the voltage is usually presented as R_p parameter [6], [36]. Practically, the R_s of the PV must be varied within 1mΩ to 1Ω, where the R_p is defined within 10Ω to 10kΩ [35]. This means that the smaller size of R_s and the larger size of R_p gain better quality of PV performance, which is shown in Fig. 7.

Therefore, the simplified and yet accurate analytical equation for R_s is determined as follows [1]:

$$R_{\mathrm{s}} = R_{\mathrm{s,ini}} - \left\{ \left[\frac{(m_{\mathrm{Tot}})\,(V_{\mathrm{t,rtc}})}{I_{\mathrm{o}}} \right] \exp\left[\frac{-V_{\mathrm{oc,stc}}}{(m_{\mathrm{Tot}})\,(V_{\mathrm{t,rtc}})} \right] \right\} \tag{6}$$

In equation (6), the R_s is a function of the ideality factor (m_{Tot}), the thermal voltage of the PV cell under real-time condition ($V_{t,rtc}$) in voltages, the reverse- saturation current of the diode (I_o) in amperes and Open-circuit voltage of the PV cell under standard test condition ($V_{oc,stc}$) in voltages. The $R_{s,ini}$ can be determined by using the slope of the I-V characteristic during I_L equals to 0. Hence,

$$R_{s,ini} = -\left(\frac{dV_L}{dI_L} \right)_{V_L = V_{oc}} \tag{7}$$

When, the $V_{t,rtc}$ can be expressed by [25], [31] and [37]:

$$V_{t,rtc} = \frac{(m_{Tot})\,(k)\,(T_c)}{q} \tag{8}$$

Consequently, the I_o is defined by [4] and [6]:

$$I_o = \frac{I_{sc,stc} + [(k_i)\,(T_a - T_{stc})]}{\left\{ \exp\left[\frac{V_{oc,stc} + [(K_V)(T_a - T_{stc})]}{(m_{Tot})(V_{t,rtc})} \right] \right\} - 1} \tag{9}$$

Where, the $I_{sc,stc}$ is the short-circuit current under standard test condition in amperes, $V_{oc,stc}$ is the open-circuit voltage under standard test condition in voltages, k_i or $dI_{sc,stc}/dT_c$ is the coefficient of the short-circuit current under standard test condition per °C in percentage and k_v or $dV_{oc,stc}/dT_c$ is the coefficient of the open-circuit voltage under standard test condition per °C in percentage are normally found in the PV manufacture datasheet. The typical values of the k_i is 3.1$\times 10^{-4}$ A/°C/cell and the k_v is -2.3$\times 10^{-3}$mV/ °C/cell [18], [25], [31], [38] and [39].

The approximation analytical equation of the R_p can be calculated as follows [40] :

$$R_p = \frac{V_{mpp,stc} + [(\mathrm{I}_{mpp,stc})\,(R_s)]}{I_l - I_o\left\{\exp\left\{\frac{q\{V_{mpp,stc}+[(\mathrm{I}_{mpp,stc})(R_s)]\}}{[(m_{Tot})(k)(T_c)]}\right\} - 1\right\} - \mathrm{I}_{mpp,stc}} \tag{10}$$

As described in equation (10), the maximum power point voltage under standard test condition ($V_{mpp,stc}$) and the maximum power point current under standard test condition ($I_{mpp,stc}$) can be obtained from the PV manufacture datasheet, and thus the photon generated current of the PV cell (I_l) depends on the solar irradiation and ambient temperature is determined as the following equation [12], [41]:

$$I_l = \{I_{sc,stc} + [(k_i)\,(T_a - T_{stc})]\}\left(\frac{G_a}{G_{stc}}\right) \tag{11}$$

2.3 Proposed a dynamic generic PV model for crystalline and thin-film technologies

Essentially, this paper proposes the dynamic generic PV model for the crystalline and thin-film technologies by applying the TFE and normalization techniques to determine the approximate ideality factor, the slope of the I-V characteristic and Kirchhoff's Current Law (KCL) considers the summation of current flow-in and flow-out of the node are chosen to estimate the R_s and R_p. The equivalent circuit of the proposed model includes a single diode, R_s and R_p are shown in Fig. 3. As the current generated by the PV (I_L) can be determined by using KCL, and hence I_L is:

$$\begin{aligned} I_L =& I_l - I_o\left\{\exp\left[\frac{q\,(V_L + I_L R_s)}{(m_{Tot})\,(k)\,(T_c)}\right] - 1\right\} \\ & - \left(\frac{V_L + I_L R_s}{R_P}\right) \end{aligned} \tag{12}$$

Therefore, the schematic of the proposed model for the computer modeling based on MATLAB/ Simulink is shown in Fig. 8.

The accurate parameters (here m_{Tot}, R_s and R_p) of the proposed model that supports either single or multi-junctions are defined by the following assumptions:

1. All the PV cells in the module have the same structure and characteristic in all manners [18], [25], [31], [38]
2. The PV module is fully illuminated [42].
3. The term of

$$\exp\left\{\frac{q\,[V_{mpp,stc} + [(\mathrm{I}_{mpp,stc})\,(R_s)]]}{[(m_{Tot})\,(k)\,(T_c)]}\right\} - 1$$

under all working conditions except low intensity light condition [43], [44].

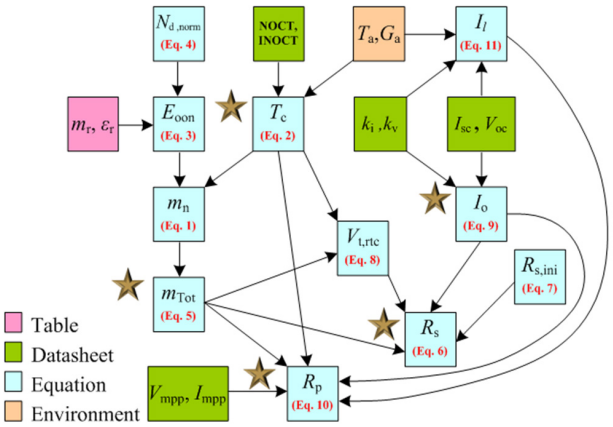

Fig. 8: *Schematic of the proposed dynamic generic PV model*

4. The impacts of the ambient temperature (T_a) and solar irradiation (G_a) on the electron potential energy between junctions, R_s and under R_p are considered, and thus the coefficient of the short-circuit current (k_i) and the coefficient of the open-circuit voltage (k_v) are also taken into account.
5. In high intensity light, the R_s for the crystalline must be less than 150 mΩ to ensure the absolute error of the proposed model within 0.05%, where the R_s can rise up to 1 Ω to support the crystalline PV with low intensity light and thin-film PV [1], [35]. Moreover, the results of significant parameters as m_{Tol}, R_s and R_p can be simulated through the schematic diagram in Fig.8. These results are shown in Table 2.

Moreover, this model supports the real-time input data of solar irradiation and ambient temperature, it can also vary the dynamic impacts of the electron potential energy between junctions, R_s and R_p. Most of the parameters are obtained from the PV manufacture datasheet. To ensure accurate simulation results of the mono-crystalline technology, the PV parameters from Bosch (model: M60EU30117 250W at 1000W/m^2 and 25°C) are chosen [45]. The simulation results of the multi-crystalline technology are also validated against the Photowatt (model: PWX100 11W at 1000W/m^2 and 25°C) [46], where the parameters of Sharp (model: NA-F121G5 142.4W at 1000W/m^2 and 25°C) is chosen to validate the simulation results of the thin-film technology [47]. The parameters of the mono-crystalline, multi-crystalline and thin-film module are shown in Table 3.

Table 2: *Parameters derived from the calculation of the proposed model.*

Parameter	Mono Crystalline	Multi Crystalline	Thin-film
	M60EU30117	PWX100	NA-121G5
$V_{oc,stc}$ (V)	37.91	21.52	60.22
$I_{sc,stc}$ (A)	8.82	0.721	3.433
$I_{mpp,stc}$ (A)	8.252	0.651	2.957
$V_{mpp,stc}$ (V)	30.32	17.01	48.2
I_o (nA)	0.183	0.057	42.4
R_s (Ω)	0.39	0.72	0.69
R_p (Ω)	632	575	236
m_{Tot}	1.05	1.1	1.96

Table 3: *Parameters of the PV module.*

Characteristic of the PV module			
Brand	Bosch	Photowatt	Sharp
Model	M60EU3017	PWX100	NA-F121G5
Type	Mono-Crystalline 60×1 parallel	Multi-Crystalline 36×1 parallel	Thin-film 45×4 parallel
$P_{mpp,stc}$ (W)	250	11.00	142.4
$V_{mpp,stc}$ (V)	30.31	17.00	48.20
$I_{mpp,stc}$(A)	8.25	0.65	2.96
$V_{oc,stc}$ (V)	37.90	21.5	60.2
$I_{sc,stc}$ (A)	8.82	0.70	3.43
k_p ($\%/°C$)	-0.46	N/A	-0.24
k_v ($\%/°C$)	-0.32	N/A	-0.30
k_i ($\%/°C$)	0.032	N/A	0.07
$NOCT(°C)$	48.4	45	44

3. RESULT AND DISCUSSION

In this section, are illustrated all the result of simulation through the proposed model, which must be compared with the other simulating model and the practical testing, are as follows:

• The other models, are composed of the existing models, such as, SDM-1, SDM 2, DDM-1 and DDM-2, respectively.

• The indoor test, which is investigated at the Solar Cells Testing Centre (CSSC) at the King Mongkut's University of Technology Thonburi in Thailand.

• The outdoor test, which this experiment is tested at the Newcastle Upon Tyne in the UK, the setting for the outdoor experimenter for PV, essentially.

Particularly, the Solar Cells Testing Centre (CSSC) at King Mongkut's University of Technology Thonburi in Thailand, set according to ISO/IEC 17025:2005. Thus, the IEC 61215:2005 [48],[49] and IEC 61646:2008 [50] was used to test the I-V characteristic of the crystalline and thin-film PV, all the materials and components of the cell was identical. The module size and the generated power did not exceed 10%. The solar simulator is a Pulsed Simulator (PS) type, and thus the flash duration was set at 10 ms and class A+A+A+ (here the error of the instability and non-uniform of intensity of light beam is less than 1.0%). This allows the accuracy measurement of the I-V test within short duration and avoids the increasing of the PV cell temperature [51]-[53].

Moreover, the proposed model was also validated with the practical site results (outdoor test) in the open area at Newcastle Upon Tyne in the United Kingdom (UK), which investigated the dynamic impacts of the surrounding environment, especially the G_a and T_a of the model. Besides, the interval data of the G_a and T_a was measured every 10 minutes via the weather data logger, the generated power of the PV was measured by multimeter. Also, Table 4 presents the details of the equipment for the indoor and outdoor tests.

3.1 The Confirmed accuracy with Indoor Test and Manufacture datasheet

For this section, the confirmation of the accuracy of the results from the proposed model will be covered. It was compared with the manufacture datasheets of PV and the indoor test data from CSSC. In this research, the three types of PV modules were studied, for instance, Mono crystalline, Multi

Table 4: *Details of the equipment for indoor and outdoor tests.*

Equipment	Model	Units	Remark
Indoor test			
Solar Simulator	Pasan: Pluse solar Simulator 3b and SunSim 3b software	1	Pulse duration 10 ms Electronic up to 300V 30A, incidence angle $<$ 15 degree, 100 to 700 W/m^2, illumined area 3m×3m
Outdoor test			
Weather logger	Davis	1	Interval data every 2s
Irradiance meter	Solar light: PMA 2200	1	Accuracy ±0.5% of Full scale reading
Thermometer	Testo: Pen style surface thermometer	1	Accuracy ±1°C of (−30°C to 250°C)
Multi-meter		1	Connect PC via USB
Power meter	Voltech: PM 1000	1	Accuracy ±0.1% of reading range
Electrical load controller	N/A	N/A	300V30A

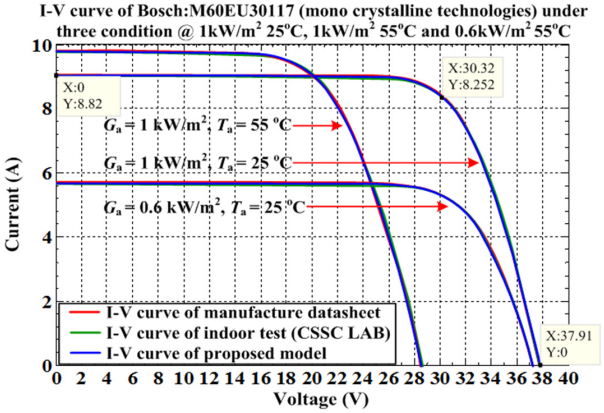

Fig.9: *I-V curve of mono-crystalline technologies at various irradiation and ambient temperatures.*

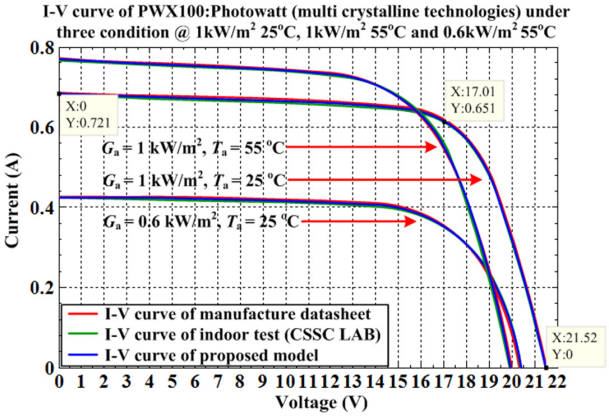

Fig.10: *I-V curve of multi-crystalline technologies at various irradiation and ambient temperatures.*

crystalline and Thin film, respectively.

As mentioned above, these are composed of the three important conditions. e.g., The first is standard test condition. The second condition is G_a= 1 kW/m^2, T_a= 55 °C and the last condition is G_a= 0.6 kW/m^2, T_a= 25 °C.

Furthermore, the results of these conditions are shown in Fig. 9 to Fig. 11, and they can be explained as follows:

In the first condition, it was analyzed from standard test conditions as G_a= 1 kW/m^2, T_a= 25 °C [45-47]. Essentially, the results of the proposed model are obviously illustrated in the characteristics current-voltage (I-V) curve as shown in Fig.9 -11, which these results show that the curve of proposed model closely matched the manufacture datasheet PV, and corresponding with the information of the indoor test.

While, the second condition is G_a = 1 kW / m^2, T_a = 55 °C. The ambient temperature in this condition is higher than the first condition. Hence, the short circuit current (I_{sc}) of the second condition is increases, while, the open circuit voltage (V_{oc}) decreases.

According to Fig. 9 to Fig. 11, the first and second condition can be demonstrated the impact of ambient temperature, which directly influence the short circuit current and the open circuit voltage, obviously. However, the I-V curve of the second condition is still extremely corresponding with the manufacture datasheet and the indoor test of CSSC, respectively.

In addition, the last condition is G_a = 0.6 kW/m^2, T_a = 25 °C, which has lower solar irradiation than other conditions. From the results, the short circuit current (I_{sc}) of this condition, decreases. Moreover, the impact of changeable by the solar irradiation, is

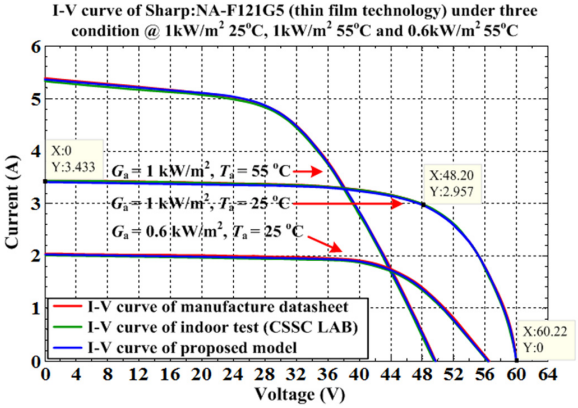

Fig.11: *I-V curve of thin-film technologies at various irradiation and ambient temperatures.*

not influenced to correspond between the result of the proposed model, the manufacture datasheet and the indoor test.

From the results in Figs. 9 to 11 can be summarized to describe as follows: All the results of the I-V curves through the proposed model in the various conditions, are closely matched to the manufacture datasheet PV, because, they have the absolute error less than 0.05%. Also, the I-V curves of the proposed are greatly consistent with the CSSC s indoor test, due to the absolute error between results no more than 0.1%. Therefore, the proposed model can deliver highly accurate result and reliable for implementation.

3.2 Comparison of results with other models

In the past several decades, the researchers have studied many models of PV modules as shown in Fig.2, such as, SDM-1 [3], SDM-2 [6], DDM-1 [9] and DDM-2 [12]. Nevertheless, all the results of the proposed model, are extremely consistent to the actual results through CCSC. While, the result of other models may only be approximate solution, as shown in Fig. 12 to Fig.13.

As shown in Fig. 12 and Fig. 13, the I-V curves of the proposed models are compared to the indoor test data from CSSC. Moreover, it is found that the results from the proposed models have less absolute error than SDM-1, SDM-2, DDM-1 and DDM-2.

Also, the many important features of the I-V curves of PV through the proposed models, is that the mean absolute error value (MAE. of I_L), is less than 0.05% from the actual results of CSSC.

Additionally, the number of iteration (n_{iter}) is lower than other models. As shown in Table 5.

Obviously, the results in Table 5 confirms the advantages of the proposed models in this article. Essentially, the I-V curve of the proposed model, is the most accurate, and has the fastest number of iteration when compared with other models. Therefore,

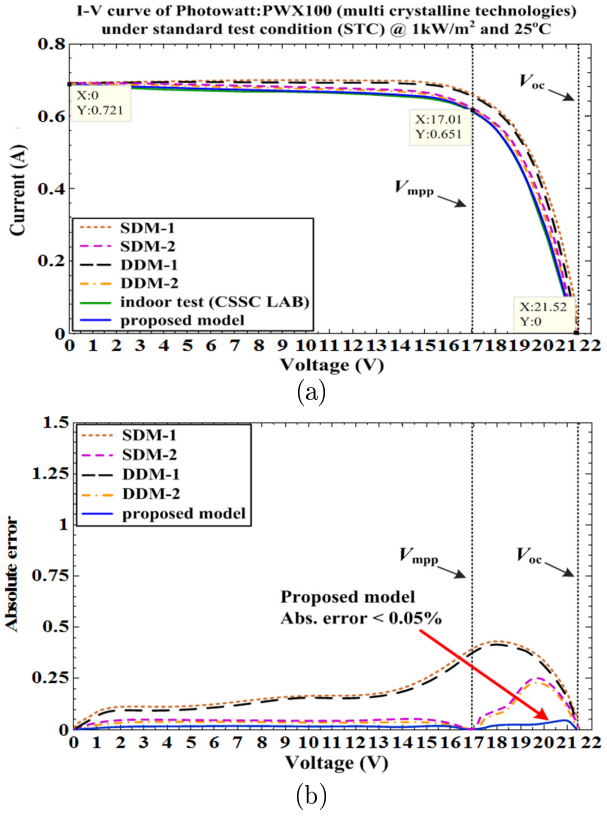

Fig.12: *Comparison of (a) the I-V Curve and (b) absolute error of PWX100 (multi-crystalline type).*

the proposed model is more suitable for applications to predict the maximum power point (mpp) of the PV module. Moreover, they can also be used to simulate the power values that vary according to the actual irradiation and ambient temperature. The next section discusses practical implementation for outdoor test.

3.3 The experimental on the outdoor test

According to Fig. 14 and 15, it shows the solar irradiation and ambient temperature can affect the output performance of PV.

Obviously, the higher ambient temperature, can decrease the generated voltage. While, the lower intensity of solar irradiation had less output of generated power. These effects are also covered to the PV with crystalline and thin film technologies, respectively.

Essentially, the thin film type NA-F121G5 of Shape, was investigated the impacts of the solar irradiation and ambient temperature with the proposed model and the outdoor test, which it can be also explained the significant parameters through (1), (2), (6) and (8) to (12).

Moreover, these relationships can be analyzed to determine the simulation results of the proposed model, which the results also agree with the manufacture datasheet and indoor test.

Table 5: *Comparison the mean absolute error of the current and the number of iteration for the five photovoltaic models at the standard test condition.*

Model	PV module					
	M60EU30117		PWX100		NA-121G5	
	n_{iter}	MAE. of I_L	n_{iter}	MAE. of I_L	n_{iter}	MAE. of I_L
SDM-1	5	0.18	4	0.21	3	0.14
SDM-2	960	0.05	585	0.07	450	0.08
DDM-1	30	0.16	20	0.19	25	0.12
DDM-2	1230	0.04	885	0.06	720	0.07
The proposed model	8	0.02	10	0.03	7	0.04

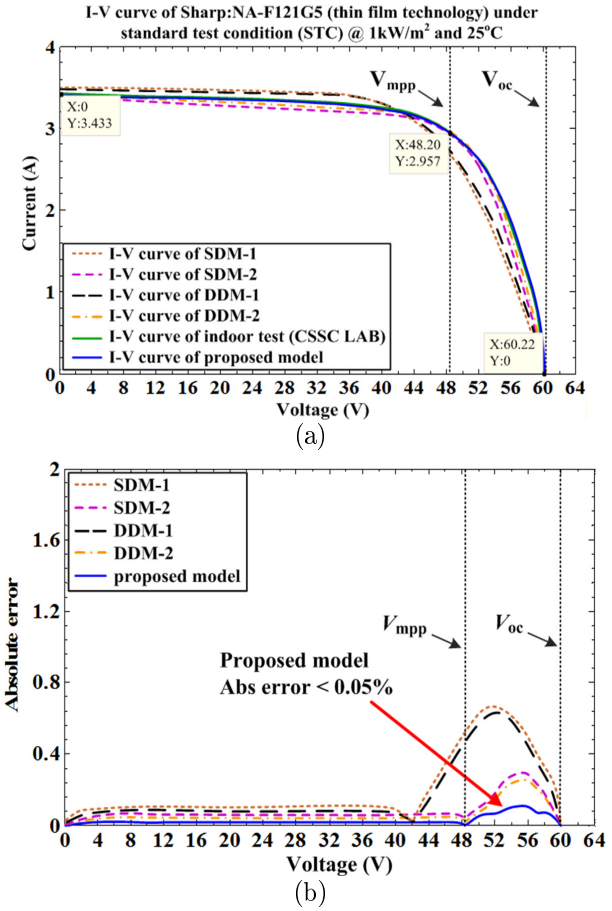

Fig.13: *Comparison of (a) the I-V Curve and (b) absolute error of NA-F121G5 (thin-film type).*

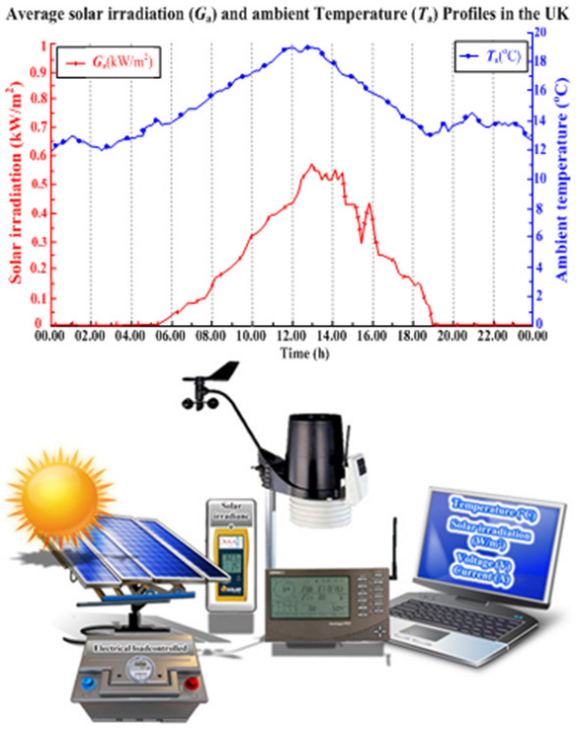

Fig.14: *Average data of Ga and Ta for one week in the UK and the setting of PV experimenter for practice.*

As mentioned above, the simulation results of the proposed model were also validated against the outdoor test. The average data of the G_a and T_a is defined by the interval data of the G_a and T_a, were measured every 10 minutes from Monday 11^{th} May 2016 to Sunday 17^{th} May 2016 (one week) at Newcastle Upon Tyne in the UK, the setting of outdoor experimenter for PV is shown in Fig. 14.

As can be seen in Fig. 14, the weather and solar irradiation data were directly transmitted to the local computer either via Wireless Fidelity (Wi-Fi), Universal Serial Bus (USB) cable or Secure Digital (SD)

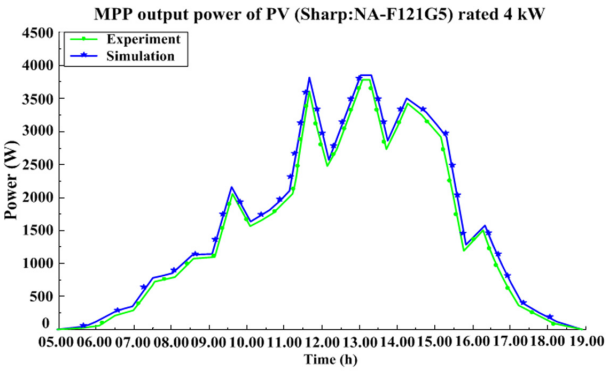

Fig.15: *Average output power of proposed model.*

card. The generated power (which is the voltage, current and power) of the PV module was measured and recorded with a multi-meter. This meter allows the data to be transferred via USB. It can be clearly seen that the solar irradiation and ambient temperature affected the performance of the PV, especially the increasing of the PV cell temperature. Therefore, an inverter that converts from Directing Current (DC) to Alternating Current (AC) and maximize the output power is needed.

According to the actual experiment results in Fig. 14, we found that a photovoltaic array type NA-F121G5 of Shape, generates the electrical power corresponded to the output of the electrical power calculated from the mathematical method of the proposed solar cell model.

As the results in Fig. 15, the comparison between the experimental results and the values calculated from the proposed model shows the maximum tolerance 15.73 watt at the following time 14.56 hours This can show that the results from the proposed models are reliable.

Furthermore, the proposed model is suitable for practical engineering applications because it can quickly calculate the results with high accuracy.

4. CONCLUSION

This paper proposed the dynamic generic model of Photovoltaic (PV) module for crystalline and thin-film technologies, which also supports the dynamic real-time input data of solar irradiation and ambient temperature using the MATLAB/Simulink program. The input parameters of the model were mostly obtained from the PV manufacture datasheet, where the specific data such as the density concentration of the ionized donor (N_d), the effective mass of the donor electron (m_s) and the relative permittivity or dielectric constant of donor material (ε_r)were also defined from the composite material properties table. The proposed model uses Thermionic Field Emission (TFE) and normalization techniques to determine the ideality factor, which is a function of the junction PV cell temperature and the N_d.

The three typical PV modules used to validate against the mono-crystalline, multi-crystalline and thin-film technologies were Bosch (model: M60EU30117 250W at 1000W/m^2 and 25°C), Photowatt (model: PWX100 11W at 1000W/m^2 and 25°C) and Sharp (model: NA-F121G5 142.4W at 1000W/m^2 and 25°C), respectively. The results showed that the I-V characteristic of the proposed model was similar to the PV manufacture datasheet.

To implement the proposed model into practice, the results were also validated against the laboratory and practical data, respectively. Therefore, the laboratory data from the Solar Cells Testing Centre (CSSC) at King Mongkut's University of Technology Thonburi in Thailand was chosen. This is due to the laboratory was set according to ISO/IEC 17025:2005, the IEC 61215:2005 and IEC 61646:1996 standards were selected as they allow the terrestrial test of crystalline silicon and thin-film PV modules. However, the practical site data from Power and Wind Energy Research (PaWER) at Northumbria University in the UK was used to achieve the accuracy of the proposed model. The results of the proposed model also matched the laboratory and practical data, when the percentage of absolute error between the proposed PV model, the laboratory data and the practical site data were less than 0.1%.

5. REFERENCES

References

[1] D. S. H. Chan and J. C. H. Phang, "Analytical method for the extraction of solar cell single and double diode model parameters from i-v characteristics," *IEEE Trans. Electron. Devices*, vol. 34, pp. 286-293, Mar. 1987.

[2] W. Xiao, W.G. Dunford and A. Capel, "A novel modeling method for photovoltaic cells," *Proc. IEEE on Power Electron. Specialists Conference* , 2004, pp. 1950-1956.

[3] G. Walker, "Evaluating mppt converter topologies using a matlab pv model," *Int. J. elect. electron. eng.*, vol. 21, pp. 1-6, 2001.

[4] R. Khezzar, M. Zereg and A. Khezzar, "Modeling improvement of the four parameter model for photovoltaic modules," *Solar Energy*, vol. 110, pp. 452-462, Nov. 2014.

[5] D. Sera, R. Teodorescu and P. Rodriguez, "PV panel model based on datasheet values," *Proc. IEEE Int. Conference Symp. Ind. Electron.* , 2007, pp. 2392-2396.

[6] M. G. Villalva, J. R. Gazoli and E. R. Filho, "Comprehensive approach to modeling and simulation of photovoltaic arrays," *IEEE Trans. Power Electron.*, Vol. 24, No. 5, pp. 1198-1208, May. 2009.

[7] F. Ghani, G. Rosengarten, and M. Duke, "The characterisation of crystalline silicon photovoltaic devices using the manufacturer supplied data," *Solar Energy*, Vol. 132, 2007, pp. 15-24, Jul. 2016.

[8] K. Hellali, "Modelisation d'une cellule photovoltaique : etude comparative," M.S. thesis, Universite Mouloud Mammride Tizi Ozou, 2012.

[9] M. Azzouzi, L. Iaeng Mazzouz and D. Popescu, "Matlab-simulink of photovoltaic system based on a two - diode model," *Proc. World Congr. Eng.* , 2014, pp. 2-4.

[10] M. Wolf and H. Rauscheback, "Series resistance effects on solar cell measurements," *Advanced Energy Conv.*, Vol. 3, No. 2, pp. 455-479, Apl.-Jun. 1963.

[11] J. A. Gow and C. D.Manning, "Development of a photovoltaic array model for use

in power-electronics simulation studies," *Proc. IEE-Electric Power Applicat.*, pp. 193-200, Mar. 1999.

[12] K. Ishaque, Z. Salam and H. Taheri, "Accurate matlab simulink pv system simulator based on a two-diode model," *IEEE Trans. Power Electron.*, Vol. 11, No. 2, pp. 179-187, Mar. 2011.

[13] E. F. Fernandez, J. Montes-Romero, J. Casa, P. Rodrigo and F. Almonacid, "Comparative study of methods for the extraction of concentrator photovoltaic module parameters," *Solar Energy*, Vol. 137, pp. 413-423, Aug. 2016.

[14] S. Shong we and M. Hanif Moin, "Comparative analysis of different single-diode pv modeling methods," *IEEE Trans. Photovoltaic*, Vol. 5, No.3, pp. 938-946, May 2015.

[15] M. S. Abdul Kareem and M. Saravanan, "A new method for accurate estimation of pv module parameters and extraction of maximum power point under varying environmental conditions," *Turkish J. Elect. Eng. Comput. Sci.*, Vol. 24, No. 4, pp. 2028-2041, Apl. 2016.

[16] E. H. Rhoderick and R. H.Williams, *Metal-semiconductor contacts*, Oxford University Press, United Kingdom, 1988.

[17] M. K. Fuentes, *A simplified thermal model for flat-plate photovoltaic arrays*, Sandia National laboratories, United State of America, 1987.

[18] P. Suwanapingkarl. *"Power quality of analysis of future power network," Ph.D.dissertation, Northumbria University, Newcastle.* [Online]. Available: http://nrl.northumbria.ac.uk/12625/1/suwanapingkarl.pasist_phd.pdf

[19] P. Hersch and K. Zweibel, *Basic photovoltaic principles and methods*, Printed in the United States of America, 1981.

[20] W. Shockley, "The theory of p-n junction in semiconductors and p-n junction in transistors," *Bell syst. Tech. J.*, Vol. 28, No. 3 pp. 435-489, Jul. 1949.

[21] G.H. Parker. *Tunneling in Schottky barriers. Ph.D.dissertation, California Institute of Technology, California.* [Online]. Available: http://resolver.caltech.edu/CaltechETD:etd-06212004-113629

[22] J. R. Hauser, and P. M. Danbar, *"A theoretical anal. of the current-voltage characteristics of solar cells (NASA-CR-138828,"* United Stage of America, The national Aeronautics and Space administration (NASA). 1974.

[23] F. A. Padovani and R. Stratton, "Field and themionic-field emission in Schotty bariers," *Solid-State Electron.*, Vol. 9, No.7, pp. 695-707, Jul. 1966.

[24] M. K. Hudait and S. B. krupanidhi, "Doping dependence of the barrier height and ideality factor of Au/n-GaAs Schottky diodes at low temperature," *J. Physica B. Condensed matter.*, Vol. 307, pp.125-137, Dec. 2001.

[25] M. A. Green, *"Solar cells: operating principles, tech. and syst. applicat.,"* Englewood Cliffs., Prentrice-Hall, 1982.

[26] C. T. Kroll and S. Wolfl Ranking, "A closer look on globalisation method for normalisation gene expression arrays," *Nucleic Acid Res.*, Vol. 30, No. 11, pp. e50, 2002.

[27] K.F.Young and H. P. R. Frederikse, "Compilation of the static dielectric constant of inorganic solids," *J. Physical Chemical Reference Data 2*, Vol. 2, No. 2, pp. 313-410, 1973.

[28] M. Bashahu and P. Nkundabakura, "Review and tests of methods for the determination of the solar cell junction ideality factors," *Solar Energy*, Vol. 81, No.7, pp. 856-863, Jul. 2007.

[29] A. Garcia-Rivera, E. comesana, A. J. Garcia-loureior, R. Valin, J.A. Rodriguez and M. Vetter, "Simulation of a-Si:H dual junction solar cells," *Proc. IEEE Spanish Conference Electron. Device* , 2013, pp.373-376.

[30] S. Y. Kuo, M. Y. Hsieh, D. H. Hsieh, H. C. Kuo and F. I. Lai, "Devices modeling of the performance of Cu(In,Ga)Se2 solar cells with v-shaped bandgab profile," *Int. J. Photo energy Article ID 186579*, pp. 1-6, Jul. 2014.

[31] W. Shockley and H. J. Queisser, "Detailed balance limit of efficiency of p-n junction solar cells," *J. Appl. Physic*, Vol. 32, No. 3, pp. 510-519, Jun. 1961.

[32] M. A. Green, "General solar cell curve factor including the effect of ideality factor, temperature and series resistant," *Solid-State Electron.*, Vol. 20, No. 3, pp. 265-266, 1977.

[33] H. L. Tsai, "Insolation-Oriented model of photovoltaic module using Matlab/Simulink," *Solar Energy*, Vol. 84, No. 7, pp. 1318-1326, Jul. 2010.

[34] L. Kennerud Kenneth, "Analysis of performance degradation in CdS solar cell," *IEEE Trans. Aerospace Electron. Syst.* , Vol. AES-5, No. 6, pp. 912-917, Dec. 1969.

[35] M. M. Subry and A. E. Ghitas, "Influence of temperature on method for determining silicon solar cell series resistance," *J. Solar Energy Eng.*, Vol. 129, pp. 331-335, Aug. 2007.

[36] A. Emerson, C. Fabricio Bradaschia Marcelo Cavalcanti J. Aguinaldo and Jr. Nascimento, "Parameter Estimation Method to Improve the Accuracy of Photovoltaic Electrical Model," *IEEE Trans. Photovoltaics*, Vol. 6, No.1, pp. 278-285, Oct. 2016.

[37] D. H. Muhsen, A. B. Ghazali, T. Khatib and I. A. Abed, "Extraction of photovoltaic module model's parameters using an improved hybrid differential evolution / electromagnetis m-like algorithm," *Solar Energy*, Vol. 119, pp. 286-297, Dec. 2015.

[38] M. A. Green, "Solar cell fill factors: general graph and empirical expressions," *Solid-State Electron.*, Vol. 24, No. 8, pp. 788-789, 1981.

[39] S. R. Wenham, M.A. Green, M.E. Watt and R. Corkish, *"Appl. photovoltaics,"* Englewood Cliffs., TJ International Ltd., UK, 2007.

[40] H. Bellia, R. Youcef, and M. Fatima, "A detailed modeling of photovoltaic module using MATLAB," *J. Astronomy Geophysics*, Vol. 3, No.1, pp. 53-61, Jun. 2014.

[41] A. Orioli and A. Di, Gangi, "A procedure to calculate the five-parameter model of crystalline silicon photovoltaic Modules on the basis of the tabular performance data," *Appl. Energy*, Vol. 102, pp. 1160-1177, Feb. 2013.

[42] M. S. Swaleh and M. A. Green, "Effect of shunt resistance and bypass diodes on the shadow tolerance of solar cell modules," *Solar Cells*, Vol. 5, pp. 183-198, Jan. 1982.

[43] C. M. Singal, "Analytical expressions for the series-resistance-dependent maximum power point and curve factor for solar cells," *Solar Cells*, Vol. 3, pp. 163-177, Mar. 1981.

[44] A.D. Vos, "The fill factor of a solar cell from a mathematical point of view," *Solar Cells*, Vol. 8, pp. 283-296, Apr. 1983.

[45] *Bosch-solar energy. Bosch solar module c-Si M60.* [Online]. Available: http://www.neutek-energy.com.au/bosch-solar/bosch-solar-module-c-si-m-60

[46] G.H. Parker. *Photowatt. Photowatt PWX 100.* [Online]. Available: http://www.proidea.hu/bps-business-power-systems-107698/photowatt-napelemek-252476/PW%20X100.pdf

[47] G.H. Parker. *Sharp. Sharp NA-F121 (G5).* [Online]. Available: http://www.gehrlicher.com/fileadmin/content/pdfs/en/modules/Sharp_NA-F121_en.pdf

[48] *"SimPowerSystems User's Guide for Use with Simulink R2014a.,"*Hydro-Quebec and TransEnergie Technologies.,

[49] *The International Electrotechnical Commission (IEC). 2005. International standard for IEC Std. 61215, Crystalline silicon terrestrial photovoltaic (PV) modules-design qualification and type approval.* IEEE Std. 61215-2005-04, (edn.2).

[50] *The International Electrotechnical Commission (IEC). 2008. International standard for IEC Std. 61646, Thin-film terrestrial photovoltaic (PV) modules-design qualification and type approval.* IEEE Std. 61646.

[51] D. Chenvidhya, T. Srisaksomboon and M. Seapan, "Test report PV modules performance (CSSC/PV/075)," Thailand, Rep., CES Solar Cell Testing Center (CSSC).

[52] W. Marion, A. Anderberg, C. Deline, S. Glick, M. Muller, G. Perrin, J. Rodriguez, S. Rummel, K. Terwilliger and T. J. Silverma. "User's manual for data for validating models for PV module performance (NREL/TP-5200-61610)," United States of America,: The National Renewable Energy Laboratory (NREL).

[53] Meyer burger. *Pasan Solar simulator. Pulse solar simulator 3b and SunSim 3b software.* [Online]. Available: http://www.eurac.edu/en/research/technologies/renewableenergy/publications/Documents/SolaRE-PV_Flyer_EN.pdf

Kotchapong Sumanonta was born in Bangkok, Thailand, in 1976. He received the B.Eng. degree in Electronic Engineering from Rajamangala University of Technology Thanyaburi (RMUTT), Pathum Thani, in 1998, where he succeeded in getting the MSc. degree in Electrical Control System and Instrument Engineering from King Mongkut' University of Technology Thonburi (KMUTT) , Bangkok, in 2005. He currently toward studying a Ph.D. degree at King Mongkut' University of Technology North Bangkok (KMUTNB). His current research interested power electronics for solar energy conversion and PV modelling.

Pasist Suwanapingkarl received B. Eng. Degree in Electrical Power Engineering from King Mongkut's University of Technology Thonburi (KMUTT), Bangkok, Thailand, where he succeeded in getting the MSc. degree and Ph.D. degree in Electrical Power Engineering from Northumbria University, Newcastle, UK. He also attained an Associate Engineer of Electrical Engineering of Thailand from Council of Engineers Thailand. Now, he has been worked at the Department of Electrical Engineering, Faculty of Engineering at Rajamangala University of Technology Phra Nakhon (RMUTP) since 2012. Moreover, he has been worked at Effiplus Co., Ltd. with engineering director position. He received the young researcher award 2015 from RMUTP. His researches mainly interested in Renewable Energy, Energy Conversion, Power Plant and Substation, Power System, Power Quality (PQ) and Grounding System.

Pisit Liutanakul was born in Bangkok, Thailand, in 1975. He received the B.Eng. and M.Eng. degrees from King Mongkut's Institute of Technology North Bangkok (KMITNB) where is now King Mongkut's University of Technology North Bangkok (KMUTNB), Thailand, in 1998 and 2002, respectively, and the Dr.-Ing. degree from Institut National Polytechnique de Lorraine (INPL), Vandoeuvre-les-Nancy, France, in 2007, all in electrical engineering. From 1998 to 1999, he worked as an engineer at Piller (Thailand) Co., Ltd. From 2007 to 2013, he taught circuit theory, analogue electronics, and automatic control systems. Since 2014, he has been involved as an Associate Professor at KMUTNB, Thailand. His research interests include stability analysis of DC-Distributed Power Systems (DC-DPSs) under the integration of multi-source/multi-load, harmonics in power system, power-factor correction, PV modeling, modeling and control of PWM DC-DC converters. He is a co-director of Green energy Research Group (GRG), whose main research fields are power electronics applications.